Phosphorus and the roles of productivity and nutrient recycling during oceanic anoxic event 2

Haydon P. Mort*, Thierry Adatte, Karl B. Föllmi — Institute of Geology, University of Neuchâtel, Rue Emile Argand 11, Case postale 158, CH-2009 Neuchatel, Switzerland
Gerta Keller — Department of Geosciences, Princeton University, Guyot Hall, Princeton, New Jersey 08544-1003, USA
Philipp Steinmann, Virginie Matera — Institute of Geology, University of Neuchâtel, Rue Emile Argand 11, Case postale 158, CH-2009 Neuchatel, Switzerland
Zsolt Berner, Doris Stüben — Institut für Mineralogie und Geochemie, Universität Karlsruhe, 76128 Karlsruhe, Germany

ABSTRACT

Four sections documenting the impact of the late Cenomanian oceanic anoxic event (OAE 2) were studied in basins with different paleoenvironmental regimes. Accumulation rates of phosphorus (P) bound to iron, organic matter, and authigenic phosphate are shown to rise and arrive at a distinct maximum at the onset of OAE 2, with an associated increase in $\delta^{13}C$ values. Accumulation rates of P return to pre-excursion values in the interval where the $\delta^{13}C$ record reaches its first maximum. An offset in time between the maximum in P accumulation and peaks in organic carbon burial, hydrogen indices, and C_{org}/P_{react} molar ratios is explained by the evolution of OAE 2 in the following steps. (1) An increase in productivity increased the flux of organic matter and P into the sediments; the preservation of organic matter was low and its oxidation released P, which was predominantly mineralized. (2) Enhanced productivity and oxidation of organic matter created dysoxic bottom waters; the preservation potential for organic matter increased, whereas the sediment retention potential for P decreased. (3) The latter effect sustained high primary productivity, which led to an increase in the abundance of free oxygen in the ocean and atmosphere system. After the sequestration of CO_2 in the form of black shales, this oxygen helped push the ocean back into equilibrium, terminating black shale deposition and removing bioavailable P from the water column.

Keywords: phosphorus, feedbacks, biogeochemistry, Cenomanian-Turonian, oceanic anoxic event 2.

INTRODUCTION

Periods during which oceanic bottom waters became oxygen depleted are well documented for the Cretaceous, and their study has led to an improved understanding of the global carbon cycle and climate change in a greenhouse world (Schlanger and Jenkyns, 1976; Jenkyns, 1980). The late Cenomanian oceanic anoxic event (OAE 2) is one of the most prominent anoxic episodes of the Mesozoic, characterized by the widespread accumulation of organic-carbon rich sediment and diagnostic redox-sensitive metals (e.g., Orth et al., 1993). OAE 2 was accompanied by a 2‰ positive $\delta^{13}C$ excursion in marine carbonates and organic matter with a plateau of high $\delta^{13}C$ values that persisted during the anoxic episode. Biotic effects resulting in the extinction as well as the evolution of new species are clearly observed (e.g., Leckie, 1985). Various OAE triggering mechanisms have been proposed, ranging from increased oceanic CO_2 derived from large igneous province activity (Kerr, 1998) to the increased nutrient delivery into surface waters from continental sources (e.g., Larson and Erba, 1999). However, there are large gaps in our understanding of these events, particularly with respect to the rate of primary productivity, its interactions with the global nutrient cycles, and feedback mechanisms caused by O_2-deficient bottom waters. This study focuses on the behavior of phosphorus (P) during OAE 2, in order to evaluate the roles of primary productivity and nutrient cycling and to test the outcome of numerical models by Van Cappellen and Ingall (1994, 1996), in which a relationship is postulated between anoxic conditions, P regeneration, and sustained primary productivity.

The behavior of the carbon and P cycles during OAE 2 are reconstructed in four localities representative of differing paleoceanographic regimes, based on whole-rock stable carbon isotopes, quantities and types of organic matter, and phosphorus mass accumulation rates (P MARs) for P bound to oxyhydroxides, authigenic minerals, detrital material, and organic matter. The sections studied are at Pueblo (Colorado, USA), Eastbourne (UK), Furlo (Italy), and Manilva (Spain). The Pueblo section is located in the relatively shallow Western Interior Seaway and, as the Cenomanian-Turonian stratotype section and point, forms a reference point for dating other sections based on high-resolution planktic foraminiferal biostratigraphy and the typical $\delta^{13}C$ record for OAE 2 (Fig. 1, Site 1) (Keller et al., 2004). A new chronostratigraphic framework was applied to the Pueblo section (Sageman et al., 2006) generating relative ages based on orbital frequencies identified above bed 63 (see Pueblo bed number in Fig. 2). The Eastbourne section (Site 2) was deposited in a continental shelf setting and has also been studied extensively (e.g., Paul et al., 1999; Gale et al., 2005). The sections at Furlo (Site 3), located in the Umbria-Marche Basin, Italy, and Manilva (Site 4), in Andalusia, southern Spain (Reicherter et al., 1994), were deposited in deep pelagic environments marked by organic-rich deposition (i.e., the Bonarelli level; Luciani and Cobianchi, 1999).

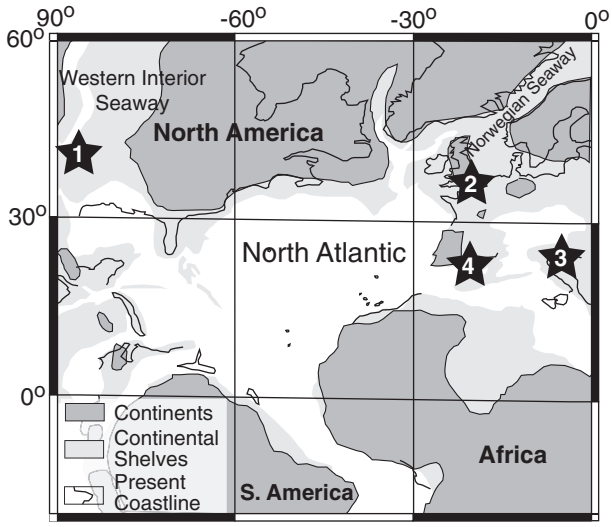

Figure 1. Paleogeography of western Northern Hemisphere at Cenomanian-Turonian boundary (93.5 Ma). Adapted from Kuypers et al. (2002). Study sites: 1—Pueblo, 2—Eastbourne, 3—Furlo, 4—Manilva.

*E-mail: haydon.mort@unine.ch

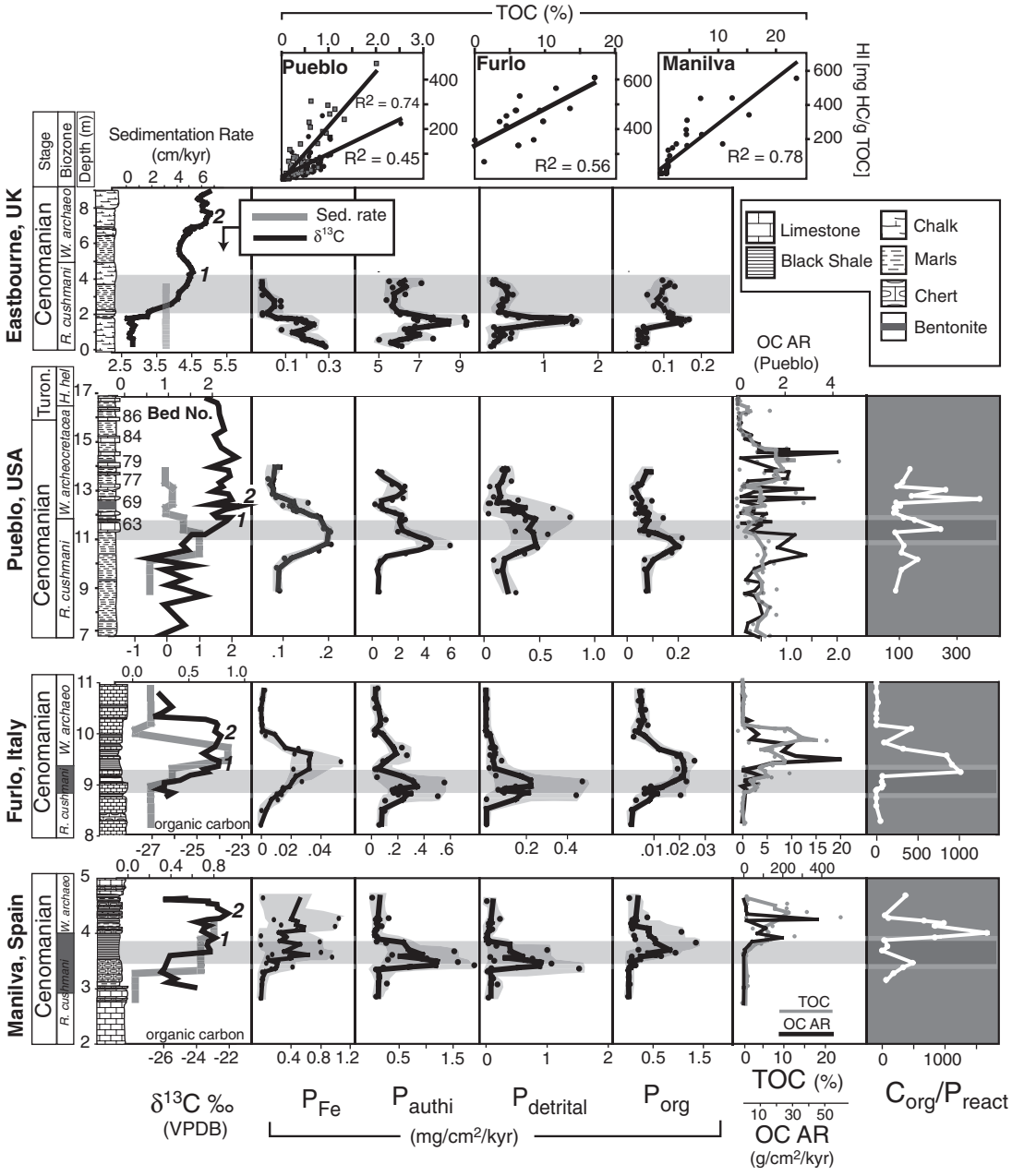

Figure 2. Phosphorus (P) speciation with accumulation rates (mg/cm²/k.y.) in four sections, plotted against corresponding $\delta^{13}C$ curves. Gray shaded area highlights interval in time between peak in P mass accumulation rates and first peak in $\delta^{13}C$ values. Percentages for total organic carbon, hydrogen indices, and $C_{org}/P_{reactive}$ molar ratios are also shown. Smoothed lines are 3-point moving averages. Scatter plots are correlations between total organic carbon (TOC) and hydrogen indices. Two correlations are made for Pueblo (black circles and gray squares represent terrestrial and/or oxidized and marine organic matter, respectively). *Rotalipora cushmani* biozones in Furlo and Manilva are extended with gray bars, which represent probable extinction level. All P speciation data can be found in Appendix 1 (also see Appendix 2 for more details; see footnote 1). Tur.—Turonian; OC AR—organic carbon accumulation rate; VPDB—Vienna Peedee belemnite.

METHODS

The SEDEX sequential extraction method (originally constructed by Ruttenberg, 1992) was used to obtain P contents for phases associated with oxyhydroxides (P_{Fe}), authigenic francolite ($P_{authigenic}$), detrital apatite ($P_{detrital}$), and organic remains ($P_{organic}$). Instrumental accuracy was <5% using a Perkin Elmer Lambda 10 spectrophometer. The P MAR was calculated in mg/cm²/k.y. Rock densities were calculated in the laboratory by measuring the displacement of water by a sample of known mass. The accumulation rates used for the Pueblo section were based on dating from Keller et al. (2004 and references therein) as well as the new cyclostratigraphic framework from Sageman et al. (2006). GSA Data Repository Appendix 1[1] contains the raw concentrations of P to enable other time scales to be used to construct MARs. Total reactive P ($P_{reactive}$) was calculated by an addition of all the measured phases, under the assumption that most detrital P represents authigenic P (Appendix 2; see footnote 1). Total organic carbon (TOC) and hydrogen indices (HI) were measured by Rock-Eval, with precisions of <1%. Molecular $C_{org}/P_{reactive}$ ratios were calculated to assess the relative importance of the vertical flux of P to and from the sediment. Intersite age control was based on the well-dated sequences at Pueblo and Eastbourne. Correlations with Furlo and Manilva were based on microfossil biostratigraphy and the $\delta^{13}C$ curves derived from organic carbon. For a more detailed methodology, see Appendix 2.

RESULTS

In all sections, concentrations and MARs of all measured P species (except for P_{Fe} in Eastbourne and P_{org} in Furlo and Manilva) reach maximum values within or close to the interval in which the onset of the $\delta^{13}C$ positive excursion is registered. They return to pre-excursion values in intervals close to those where the first peak in $\delta^{13}C$ was detected (Fig. 2).

[1]GSA Data Repository item 2007118, Appendices 1 and 2, containing raw phosphorus data, mass accumulation rates, and more detailed descriptions of the methods used in this study, is available online at www.geosociety.org/pubs/ft2007.htm, or on request from editing@geosociety.org or Documents Secretary, GSA, P.O. Box 9140, Boulder, CO 80301, USA.

The reductions in P MARs are synchronous with increases in HIs and $C_{org}/P_{reactive}$ ratios (Fig. 2). Rock-Eval data for the Eastbourne section are not available, due to the lack of organic carbon (<0.1%). In other sections, there is a positive correlation between organic carbon contents and their associated HIs. The three scatter plots in Figure 2 demonstrate this, with R^2 values of 0.78, 0.56, and 0.74 for Manilva, Furlo, and Pueblo, respectively. An improvement in the correlation is seen in the Pueblo section, above bed 63, where the origin of organic matter becomes more marine (Keller et al., 2004). At Pueblo, the organic matter content begins to increase after the first $\delta^{13}C$ peak. This is not the case at Furlo and Manilva, where TOC increased at the onset of the $\delta^{13}C$ excursion.

The section at Pueblo reveals relatively low $C_{org}/P_{reactive}$ molar ratios, with a poorly constrained peak just above the maximum in P MARs (Fig. 2). The background $C_{org}/P_{reactive}$ molar ratios in sediments below and above the organic-rich interval at Furlo are close to 1, implying a strong enrichment of P relative to TOC. The Manilva section contains higher background $C_{org}/P_{reactive}$ molar ratios (~70). In both sections, a well-defined peak in $C_{org}/P_{reactive}$ molar ratios of 1000 and 1600, respectively, is observed immediately above the interval in which P MARs decrease.

DISCUSSION

The coeval nature of the rises in P MAR during the $\delta^{13}C$ excursion at all four sections is strong evidence for the primary nature of the P signal, rather than being an artifact of changing sediment accumulation rates. The signal is therefore an expression of an important change in the marine P cycle during the onset of OAE 2. The so-called second peak in the $\delta^{13}C$ record is difficult to identify in the Furlo and Manilva sections, as in many other more pelagic environments (Tsikos et al., 2004). This difficulty means that sedimentation rates above the isotope excursion are likely to be inexact. This is unimportant to the study, which focuses on events during the onset of the isotope excursion and immediately after the first isotope peak.

Previous empirical and modeling studies have observed a decrease in P burial efficiency during periods of increased productivity (Ingall and Jahnke, 1994; Van Cappellen and Ingall, 1994). This same process is inferred here (Fig. 2). An initial increase in productivity may have reduced bottom-water O_2 availability, but not enough to prevent organic-matter degradation, which was still being oxidized (indicated by the low background $C_{org}/P_{reactive}$ molar ratios in the sections of Manilva and especially Furlo). The deeper water conditions at this stage did not impede the increase in precipitation of $P_{authigenic}$ derived from the lateral transfer of PO_4^{3-} from the oxidation of organic matter (Fig. 3, step 2). The coeval increase in $P_{organic}$ MARs is not reflected in an increase in TOC contents. This is an indication that sedimentation rate was an important control in $P_{organic}$ accumulation. Increases and decreases in HI have a positive relationship between changes in the preservation and maturity of organic matter (Demaison and Moore, 1980). Low HI values indicate that organic-matter preservation was poor during the onset of the $\delta^{13}C$ excursion and peak in $P_{reactive}$ MARs.

Increasing dysoxic bottom-water conditions related to the progressive decomposition of organic matter would have gradually inhibited the formation of $P_{authigenic}$, which makes up the bulk of P_{total} (step 4 in Fig. 3). Once this threshold was passed, $P_{reactive}$ MARs appear to have decreased. The fact that $\delta^{13}C$ continued to increase suggests that surface productivity continued without interruption, possibly sustained by the recycling of bottom-water phosphate and other redox sensitive nutrients (e.g., nitrates from the breakdown of organic matter) back into surface waters, indicated also by an increase in the $C_{org}/P_{reactive}$ ratio at the decrease in P MARs in Furlo and Manilva (step 3 in Fig. 3). This observation is ambiguous in Pueblo. Nevertheless, Pueblo, like Furlo and Manilva, shows a switch from a productivity- to preservation-driven depositional system with the increase in organic-matter content occurring after P began to reflux into the water column. Furthermore, the HIs show a good positive correlation with the TOC contents, indicating that

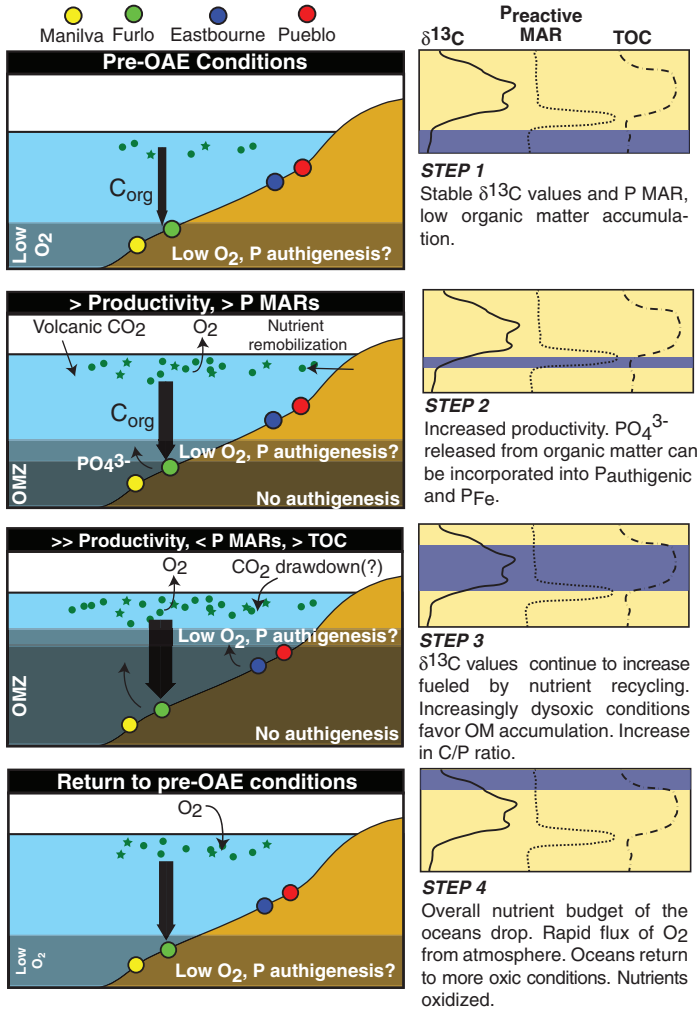

Figure 3. Schematic model to explain biogeochemical observations of this study.

preservation, not productivity, was the primary factor responsible for the accumulation of organic matter. Given good evidence that the reduction in P MAR and increases in TOC content are linked to the decreased oxygen availability, it is plausible that P recycling would create a productivity–dysoxia–nutrient recycling positive feedback loop.

The accumulation rate of $P_{organic}$ decreases with $P_{authigenic}$. The drop is less pronounced than in inorganic P phases. This indicates that sink switching from inorganic to organic matrices occurred only on a limited basis. The fact that $P_{organic}$ MAR decreases suggests that the oxidative degradation of organic matter was decelerated under slower bacterial respiration, typical in dysoxic environments (see Jorgensen, 2000, for review).

The $P_{authigenic}$ MARs in Pueblo and Eastbourne are consistently an order of magnitude higher than at Manilva and Furlo. This is likely because the latter sections record deep-water environments with lower abundances of free O_2, thus predisposing $P_{authigenic}$ production to be less efficient (Van Cappellen and Ingall, 1996; Filippelli, 1997). The P data do not extend high enough into each lithology to be sure of how OAE 2 was terminated. However, we may speculate on events that would logically play out as a result of our data.

The majority of recent studies propose that a humid climate and higher and/or rising sea levels may have reworked nutrients on previously dry land, thus stimulating the initial increase in productivity during OAE 2. A more arid environment during the $\delta^{13}C$ plateau may have reduced productivity by restricting delivery of phosphate to the sea surface (see Jarvis

et al., 2006). The decrease in productivity would be accompanied by the gradual introduction of more oxic bottom waters. In addition, enhanced primary productivity would have two effects: (1) increased the concentration of atmospheric O_2 and (2) sequestrated atmospheric CO_2, which may have been partly responsible for predisposing the oceans to anoxic conditions. This CO_2 may have become incorporated into organic matter, carbonate, or may have directly enhanced nutrient recycling by contributing to bottom-water dysoxia. The buildup of atmospheric O_2, produced during the enhanced primary productivity may have triggered a negative feedback, flipping the ocean into an oxic state, once a critical threshold in atmospheric O_2 concentration had been reached (Handoh and Lenton, 2003). We would therefore expect to see $P_{inorganic}$ MAR values increase toward the end of OAE 2, as the oceans became more oxic. The above factors would have worked against the productivity–anoxia–nutrient recycling feedback, returning the ocean to a pre-OAE state (step 4, Fig. 3).

CONCLUSIONS

In the investigated sections, covering the initial stages of OAE 2, P MARs reach a distinct maximum, which predates the start of the $\delta^{13}C$ positive plateau by tens of thousands of years. Together with our observations on the quality and quantity of preserved TOC and on $C_{org}/P_{reactive}$ molar ratios, we propose the following model for the evolution of the late Cenomanian OAE 2 (Fig. 3).

1. At the start of OAE 2, productivity rates increased, but initial preservation conditions remained poor for organic matter. P was liberated from organic matter during its oxidation, and simultaneously precipitated as $P_{authigenic}$ in pore waters.

2. Environmental conditions gradually became too dysoxic for $P_{inorganic}$ to form effectively. The timing of this appears to depend on the paleodepth of a given section and/or local oxygen availability. At the same time, preservation conditions for TOC improved, raising TOC contents.

3. Pore waters switched from being a P sink to a P source (indicated by an increase in $C_{org}/P_{reactive}$ ratio), sustaining the productivity-driven $\delta^{13}C$ peak and plateau in a positive feedback loop.

4. The accumulation of organic matter was strongly linked to preservation (indicated by a positive correlation with HIs).

5. Increased aridity, atmospheric O_2, content and CO_2 sequestration were all factors working against the anoxic event, bringing about a return to a more oxic water column. This idea is testable. In this paper we argue that $P_{inorganic}$ accumulation is inhibited by bottom-water oxygen depletion. A return to more oxygenated conditions would increase $P_{authigenic}$ MAR at the end of OAE 2.

ACKNOWLEDGMENTS

We thank I. Jarvis, B. Sageman, M. Arthur, P. Van Cappellen, H. Tsikos, and two anonymous reviewers for reviews. We also thank O. Jaquat and P. Ducommun, University of Neuchâtel, for collecting samples. This project was funded by Swiss National Fund (SNF) grants FN21-67702.02 and SNF 0115357.

REFERENCES CITED

Demaison, G.T., and Moore, G.T., 1980, Anoxic environments and oil source bed genesis: Organic Geochemistry, v. 2, p. 9–31, doi: 10.1016/0146–6380(80)90017–0.

Filippelli, G.M., 1997, Controls on phosphorus concentration and accumulation in oceanic sediments: Marine Geology, v. 139, p. 231–240, doi: 10.1016/S0025–3227(96)00113–2.

Gale, A.S., Kennedy, W.J., Voigt, S., and Walaszczyk, I., 2005, Stratigraphy of the Upper Cenomanian–Lower Turonian Chalk succession at Eastbourne, Sussex, UK: Ammonites, inoceramid bivalves and stable carbon isotopes: Cretaceous Research, v. 26, p. 460–487, doi: 10.1016/j.cretres.2005.01.006.

Handoh, I.C., and Lenton, T.M., 2003, Periodic mid-Cretaceous oceanic anoxic events linked by oscillations of the phosphorus and oxygen biogeochemical cycles: Global Biogeochemical Cycles, v. 17, p. doi: 10.1029/2003GB002039.

Ingall, E., and Jahnke, R., 1994, Evidence for enhanced phosphorus regeneration from marine-sediments overlain by oxygen depleted waters: Geochimica et Cosmochimica Acta, v. 58, p. 2571–2575, doi: 10.1016/0016–7037(94)90033–7.

Jarvis, I., Gale, A.S., Jenkyns, H.C., and Pearce, M.A., 2006, Secular variation in Late Cretaceous carbon isotopes: A new d13C carbonate reference curve for the Cenomanian-Campanian (99.6–70.6 Ma): Geological Magazine, v. 143, p. 561–608, doi: 10.1017/S0016756806002421.

Jenkyns, H.C., 1980, Cretaceous anoxic events, from continents to oceans: Geological Society [London] Journal, v. 137, p. 171–188.

Jorgensen, B.B., 2000, Bacteria and marine biogeochemistry, *in* Schulz, H.D., and Zabel, M., eds., Marine geochemistry: New York, Springer, p. 173–207.

Keller, G., Stueben, D., Berner, Z., and Adatte, T., 2004, Cenomanian-Turonian $\delta^{13}C$, $\delta^{18}O$, sea level and salinity variations at Pueblo, Colorado: Palaeogeography, Palaeoclimatology, Palaeoecology, v. 211, p. 19–43, doi: 10.1016/j.palaeo.2004.04.003.

Kerr, A.C., 1998, Oceanic plateau formation: A cause of mass extinction and black shale deposition around the Cenomanian-Turonian boundary?: Geological Society [London] Journal, v. 155, p. 619–626.

Kuypers, M.M.M., Pancost, R.D., Nijenhuis, I.A., and Damste, J.S.S., 2002, Enhanced productivity led to increased organic carbon burial in the euxinic North Atlantic basin during the late Cenomanian oceanic anoxic event: Paleoceanography, v. 17, article 1051, doi: 10.1029/2000PA000569.

Larson, R.L., and Erba, E., 1999, Onset of the mid-Cretaceous greenhouse in the Barremian-Aptian: Igneous events and the biological, sedimentary, and geochemical responses: Paleoceanography, v. 14, p. 663–678, doi: 10.1029/1999PA900040.

Leckie, R.M., 1985, Foraminifera of the Cenomanian-Turonian boundary interval, Greenhorn Formation, Rock Canyon Anticline, Pueblo, Colorado: Society of Economic Paleontologists and Mineralogists Bulletin, v. 4, p. 139–149.

Luciani, V., and Cobianchi, M., 1999, The Bonarelli Level and other black shales in the Cenomanian-Turonian of the northeastern Dolomites (Italy): Calcareous nannofossil and foraminiferal data: Cretaceous Research, v. 20, p. 135–167, doi: 10.1006/cres.1999.0146.

Orth, C.J., Attrep, M., Quintana, L.R., Elder, W.P., Kauffman, E.G., Diner, R., and Villamil, T., 1993, Elemental abundance anomalies in the late Cenomanian extinction interval—A search for the source(s): Earth and Planetary Science Letters, v. 117, p. 189–204, doi: 10.1016/0012–821X(93)90126-T.

Paul, C.R.C., Lamolda, M.A., Mitchell, S.F., Vaziri, M.R., Gorostidi, A., and Marshall, J.D., 1999, The Cenomanian–Turonian boundary at Eastbourne (Sussex, UK): A proposed European reference section: Palaeogeography, Palaeoclimatology, Palaeoecology, v. 150, p. 83–121.

Reicherter, K., Pletsch, T., Kuhnt, W., Manthey, J., Homeier, G., Wiedmann, J., and Thurow, J., 1994, Mid-Cretaceous paleogeography and paleoceanography of the Betic Seaway (Betic Cordillera, Spain): Palaeogeography, Palaeoclimatology, Palaeoecology, v. 107, p. 1–33, doi: 10.1016/0031–0182(94)90162–7.

Ruttenberg, K.C., 1992, Development of a sequential extraction method for different forms of phosphorus in marine sediments: Limnology and Oceanography, v. 37, p. 1460–1482.

Sageman, B.B., Meyers, S.R., and Arthur, M.A., 2006, Orbital time scale and new C-isotope record for the Cenomanian-Turonian boundary stratotype: Geology, v. 34, p. 125–128, doi: 10.1130/G22074.1.

Schlanger, S.O., and Jenkyns, H.C., 1976, Cretaceous oceanic anoxic events: Causes and consequences: Geologie en Mijnbouw, v. 55, p. 179–184.

Tsikos, H., Jenkyns, H.C., Walsworth-Bell, B., Petrizzo, M.R., Forster, A., Kolonic, S., Erba, E., Premoli-Silva, I., Baas, M., Wagner, T., and Sinninghe Damsté, J.S., 2004, Carbon-isotope stratigraphy recorded by the Cenomanian-Turonian Oceanic Anoxic Event: Correlation and implications based on three key localities: Geological Society [London] Journal, v. 161, p. 711–719.

Van Cappellen, P., and Ingall, E.D., 1994, Benthic phosphorus regeneration, net primary production, and ocean anoxia—A model of the coupled marine biogeochemical cycles of carbon and phosphorus: Paleoceanography, v. 9, p. 677–692, doi: 10.1029/94PA01455.

Van Cappellen, P., and Ingall, E.D., 1996, Redox stabilization of the atmosphere and oceans by phosphorus-limited marine productivity: Science, v. 271, p. 493–496, doi: 10.1126/science.271.5248.493.

Manuscript received 2 November 2006
Revised manuscript received 9 January 2007
Manuscript accepted 12 January 2007

Printed in USA